Study of anomalous infrared properties of nanomaterials through effective medium theory

Zhang-Fei Su,[1] Shi-Gang Sun,[1,a)] Chen-Xu Wu,[2] and Zhi-Ping Cai[3]
[1]*State Key Laboratory of Physical Chemistry of Solid Surfaces, Department of Chemistry, College of Chemistry and Chemical Engineering, Xiamen University, Xiamen 361005, People's Republic of China*
[2]*Soft Condensed Matter Laboratory, Department of Physics and ITPA, Xiamen University, Xiamen 361005, People's Republic of China*
[3]*Department of Electronic Engineering, Xiamen University, Xiamen 361005, People's Republic of China*

(Received 27 December 2007; accepted 6 June 2008; published online 28 July 2008)

Effective medium theory is introduced into a three-layer model to study the anomalous IR properties of nanostructured Pt films. A composite system is set up for the nanostructured film together with adsorbates and water around it. The anomalous IR spectral features, which exhibit a transition from enhanced (or normal) IR absorption to Fano-type bipolar line shape and, finally, to enhanced anomalous IR absorption (the abnormal infrared effects) along with the change in structure and size of nanomaterials, as observed through experiments for CO molecule adsorption, are elucidated by an increase in the volume fraction of metal in the composite system and the effective thickness of the composite system. The theoretical simulation results illustrate that the spectral line shape of IR absorption depends strongly on the volume fraction of metal, while the intensity of the IR band is directly proportional to the effective thickness. This study has revealed, through a physical optical aspect of interaction of CO molecules with nanostructured metal films, one of the possible origins of anomalous IR properties and has shed light on interpreting the peculiar properties of nanomaterials. © *2008 American Institute of Physics*. [DOI: 10.1063/1.2953441]

I. INTRODUCTION

Nanosize scale and nanostructured materials exhibit many peculiar characteristics, such as surface effect, quantum size effect, and dielectric confinement effect, and have attracted much attention in recent years for their fundamental aspects as well as valuable applications in optics, electronics, catalysis, ceramics, magnetic data storage, and other important fields.[1–3] In particular, nanostructured thin films display many special optical properties, such as surface-enhanced infrared absorption (SEIRA), surface-enhanced Raman scattering (SERS), and abnormal infrared effects (AIREs).[4–6] These anomalous optical effects are of importance in revealing the intrinsic characteristics of nanomaterials and their novel properties, thus in developing relevant theory and applications, and have become the frontier subject of multidisciplinary studies.

Lu *et al.*[6] and Sun[7] have studied systematically the AIREs of nanostructured thin films. In comparison with the normal IR spectra of CO adsorbed (CO_{ad}) on a bulk Pt surface, the IR spectra of CO_{ad} on nanostructured Pt thin films illustrated three distinct anomalous features: (1) the inversion of the direction (anomalous IR absorption) of CO_{ad} bands; (2) the significant enhancement of IR absorption; and (3) the broadening of the width of CO_{ad} bands (inhomogeneous broadening).[6] In the follow-up studies, the AIREs were also found on nanomaterials of platinum group and iron-triad metals, such as Pt, Pd, Ru, Rh, Os, Ir, Ni, Co, and their alloys on various substrates (Pt, Au, and GC).[8–15] Besides the AIREs, other two anomalous IR properties of nanostructured films are SEIRA and Fano-type IR effects that yield bipolar band features of IR absorption of adsorbates on nanostructured films.[4,16–19] With regard to studies of the origins of these anomalous IR properties, SEIRA has been attributed to the large enhancement of the incidence electric field,[20,21] which is similar to the electromagnetic (EM) mechanism introduced in interpretation of the SERS. Fano-type bipolar features may be explained by Fano resonance,[16] appearing when a discrete phonon excitation interacts with a continuum state. In the experimental aspects, we have observed the transformation between these three anomalous IR properties.[22,23] The IR features can be transformed from the enhanced (or normal) IR absorption to Fano-type bipolar line shape and, finally, to the enhanced anomalous IR absorption along with the change in the nanostructure and size of nanoparticles. These experimental results demonstrate that the anomalous IR properties are strongly correlated with the structure and size of nanomaterials. It is thus reasonable to assume that there are some intrinsic correlations behind the above-mentioned three unique IR effects, i.e., SEIRA, Fano-type and AIREs. It is worthwhile pointing out that the origin of anomalous IR properties concerns physics, chemistry, optics, and fundamental of other disciplines. Through studies of anomalous IR properties, it cannot only develop relevant theories but also reveal the intrinsic properties of nanomaterials.

Effective medium theory (EMT) provides a powerful technique to compute the optical properties of composite materials. It was first proposed by Maxwell-Garnett (MG) to

a)Author to whom correspondence should be addressed. FAX: +86 592 2183047. Electronic mail: sgsun@xmu.edu.cn.

solve the problem of colors in metal glasses one century ago.[24] From then on, there have been many extensions and revisions in literature, such as taking into account the percolation threshold,[25] the particles' shape beyond a sphere,[26] the radius of particles,[27] the interaction of dipole-dipole coupling,[28] and so on. Nowadays EMT is widely used in ultraviolet visible (UV-vis), IR, surface plasmon resonance, and many other spectroscopic studies.[8,17,20,29–31] Osawa *et al.*[20] used EMT to illuminate the SEIRA of *p*-NBA molecules adsorbed on Au nanoislands; Priebe *et al.*[17] employed EMT to simulate the asymmetric line shape in the transmission spectra of CO adsorbed on Fe thin films; and Bjerke *et al.*[8] applied the Bergman representation of EMT to interpret the SEIRA of CO adsorbed on platinized Pt. In the Bergman representation, however, the pivotal function "spectral density $g(u,l)$" that characterizes the microtopology of nanomaterials is difficult to obtain. A simulation using EMT concerning the IR spectra of CO adsorbed on nanostructured Pt thin films was reported recently by Pecharroman *et al.*[32]

To the best of our knowledge, the whole picture concerning the origins of anomalous IR properties of nanomaterials is far too completely understood. In a previous paper,[33] we have considered the interparticle interaction and the electron-hole damping between nanomaterials and CO molecules. The simulation results illuminated that the island-shaped nanostructured Pt films, which gave rise to interparticle interaction, coupling with electron-hole damping mechanism may contribute to anomalous IR properties. It is worthwhile pointing out that most of the existing theoretical studies on anomalous IR properties were mainly simulations. It should be more important to correlate the theoretical analysis using directly experimental parameters, i.e., the measured dielectric constant ε, permeability μ, and optical constants n, with experimental results. Such kind of investigation may reveal the intrinsic properties of nanomaterials.

In this paper, EMT is introduced into a three-layer model to formulate the simulation of the IR spectra of CO adsorbed on the Pt nanostructured thin films. All the spectra depend on two parameters, which are convenient to fit the simulation results with the experimental data. The results presented in this paper have revealed the relationship between the anomalous IR properties and the surface structure of nanomaterials, and has shed light in acquiring new knowledge on nanomaterials.

II. THEORETICAL MODEL AND EXPERIMENT

Figure 1(a) is the schematic presentation of our experimental system. In experiment, the lowest layer is the substrate, such as Pt, Au, or GC. On the substrate, a thin layer of metal nanoparticles is grown using electrochemical methods. The nanoparticles, covered by a layer of adsorption molecules, are immersed in water, which is the second layer. The upmost layer is water. In our theoretical studies, a three-layer model, shown in Fig. 1(b), is used to simulate the practical system in which the first layer is water, the third layer is the substrate, and the layer between them is an effective layer composed of metal nanoparticles and other molecules.

For each layer, an optical constant is given to describe its

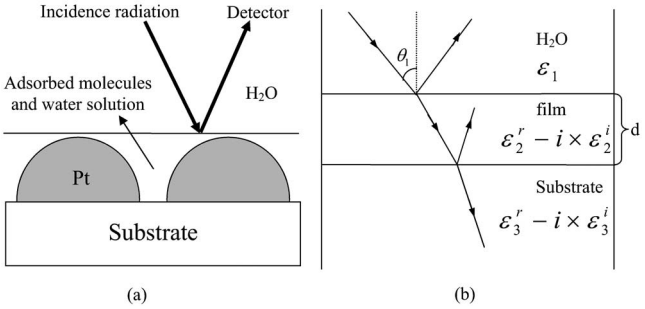

FIG. 1. Schematic representations of (a) experimental system and (b) three-layer theoretical model.

optical property. The refractive index of water is $1.316-0.016\times i$ (in $1900\sim2200$ cm^{-1} region),[34] and the refractive index data of Pt are obtained from Ref. 35. We have plotted the real part and the imaginary part of refractive index of Pt versus wave numbers between 1900 and 2200 cm^{-1}, and obtained a linear relationship that was used ultimately in the simulation. The dielectric constant can be calculated as the square of refractive index. Since the size of metal nanoparticles is much smaller than the wavelength of IR incidence light, EMT has to be used to calculate the effective dielectric constant of the second layer composed of Pt nanoparticles and other molecules, which are treated in this paper as a homogeneous medium. Strictly speaking, the second layer consists of three phases: Pt nanoparticles, CO molecules, and water. A consideration of the three phases separately will cause the simulation many complications. As an approximation in our study, CO molecules and water are treated as a "mixed phase," and Pt nanoparticles are immerged in this mixed phase. When no CO adsorption takes place, the mixed phase is simply water with a real-number dielectric constant, and the CO adsorption only adds an imaginary part to this dielectric constants. According to the *D*-dimensional Bruggeman EMT,[36] the effective dielectric constant satisfies

$$f\frac{\varepsilon_m-\varepsilon_{\text{eff}}}{\varepsilon_m+(D-1)\varepsilon_{\text{eff}}}+(1-f)\frac{\varepsilon_{\text{mix}}-\varepsilon_{\text{eff}}}{\varepsilon_{\text{mix}}+(D-1)\varepsilon_{\text{eff}}}=0, \qquad (1)$$

where $D=2$ stands for two-dimensional arrangement of Pt nanoislands,[17] ε_{eff} is the effective dielectric constant of the homogeneous medium, ε_m and ε_{mix} are the dielectric constants of metal and mixed phase, respectively, and f is the volume fraction of metal in the homogeneous medium. f ranges between 0 and 1. If f equals 0, it refers to mixed phase on bulk metal surface without metal nanoparticles, while if f equals 1, it means only bulk metal without mixed phase; when $0<f<1$, it signifies metal nanoparticles on the mixed phase.

The dielectric constant of the mixed phase can be represented by the Lorentz harmonic oscillator, which is given by[20]

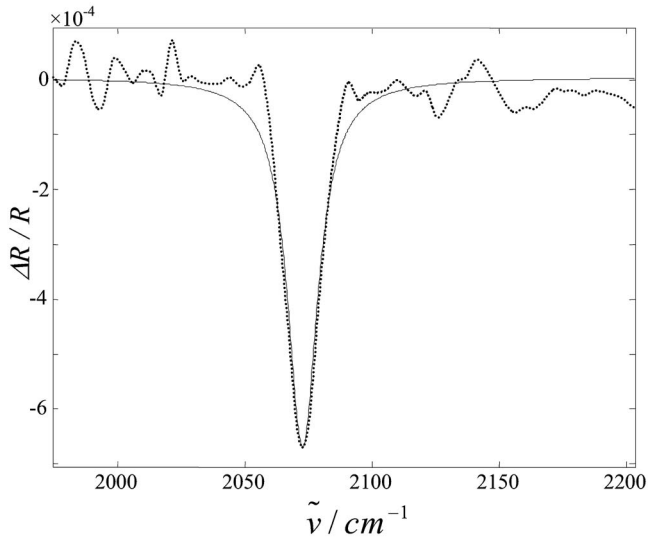

FIG. 2. Experimental and simulated IR spectra of CO adsorbed on bulk Pt surface. Dotted line: experimental; solid line: simulated.

$$\varepsilon_{\text{mix}} = \varepsilon_r - i\varepsilon_i,$$

$$\varepsilon_r = n_\infty^2 + \frac{B(\nu_0^2 - \nu^2)}{(\nu_0^2 - \nu^2)^2 + \gamma^2\nu^2}, \tag{2}$$

$$\varepsilon_i = \frac{B\gamma\nu}{(\nu_0^2 - \nu^2)^2 + \gamma^2\nu^2},$$

where ν is the frequency in wave number (cm^{-1}), ν_0 is the peak center of CO band, n_∞ is the refractive index of mixed phase far away from ν_0, γ is the full width at half maximum of CO band, and B is a parameter that determines the intensity of CO band. All the complex dielectric constants used in this paper are expressed by $\varepsilon_r - i\varepsilon_i$ ($\varepsilon_i \geq 0$), where ε_r and ε_i are the real and the imaginary parts, respectively. The parameters in the dielectric constant of "mixed phase" can be measured by the reflective spectrum of CO adsorbed on smooth Pt surface. Figure 2 shows the experimental and the simulated IR spectra of CO adsorbed on bulk Pt surface. From experimental spectrum we obtain $\nu_0 = 2070\ \text{cm}^{-1}$ and $\gamma = 14.5\ \text{cm}^{-1}$, and a numerical fitting through MATLAB software leads to $n_\infty = 1.66$ and $B = 30\,000$.

From Eq. (1), the effective dielectric constant can be written as

$$\varepsilon_{\text{eff}} = (f - 0.5)(\varepsilon_m - \varepsilon_{\text{mix}}) \mp \sqrt{(f - 0.5)^2(\varepsilon_m - \varepsilon_{\text{mix}})^2 + \varepsilon_m \times \varepsilon_{\text{mix}}}. \tag{3}$$

The sign "–" or "+" is chosen to make sure that the imaginary part of ε_{eff} is positive.

The electrochemical preparation of nanostructured Pt thin films was conducted on an electrochemical work station (CHI 631C). The potentials were quoted versus a saturated calomel electrode. All solutions were prepared using Milli-Q water, H_2SO_4 of super pure, and K_2PtCl_6 of analytical grade. The surface structures of nanostructured Pt films were investigated using scanning tunneling microscopy (STM) of type P4–18-SPM (NTMDT, Russia). The *in situ* Fourier transform infrared (FTIR) experiments were carried out on a Nexus 870 FTIR spectrometer (Nicolet).

The experimental FTIR spectra are represented as the relative change in reflectivity by

$$\frac{\Delta R}{R} = \frac{R(E_S) - R(E_R)}{R(E_R)}, \tag{4}$$

where $R(E_S)$ and $R(E_R)$ are the single-beam spectra of reflection collected at sample potential E_S and reference potential E_R, respectively. In the experiment, E_R is set at the potential where CO is completely oxidized and E_S is chosen for those potentials at which CO is stably adsorbed on the Pt surface. Under these conditions, the features of CO_{ad} band in the spectra are exclusively IR absorption of CO_{ad} species at E_S.

According to the STM result, the thickness of the nanostructured thin films is much smaller than the wavelength of IR radiation; hence, the relative change in IR reflectivity can be simulated by the three-layer structure simplification.[37] The choice of reference spectra does not affect the shape and intensity of the CO band, both the reflective spectra of bulk Pt surface and of nanostructured Pt films can be used as reference spectra. However, in order to ensure the straightness of baseline, the reflective spectra of nanostructured Pt films without CO adsorption are used as the reference spectra, which can be simulated according to the dielectric constants of Pt and water. The incidence angle is set as 60°, which is the same angle used in experimental studies. The simulations were carried out for the IR spectra collected by *s*- and *p*-polarization light, respectively, for CO molecules adsorbed on bulk Pt surface. In the case of *p*-polarization light, the calculated signal is about 10^{-3}, while the signal is less than 10^{-5} for *s*-polarization light, which is too weak to be detected by IR measurements. As a consequence in simulations conducted in the present paper, we have used only the *p*-polarization light as incidence. All the simulations in this paper are carried out using MATHEMATICA software.

III. RESULTS AND DISCUSSION

Figure 3(a) shows the *in situ* FTIR spectra of CO molecules adsorbed on the nanostructured Pt thin films based on the Pt surface. The thin films are prepared by oxidation-reduction cycling (ORC) on K_2PtCl_6 solution for different treatment times. It is found that on untreated (bulk) Pt surface, the CO band is a symmetric and negative-going band, which can be assigned to the normal IR absorption of linear adsorbed CO species (CO_L) on the Pt surface. When CO molecules adsorb on the Pt thin film prepared by ORC for 20 min, a Fano-type bipolar band with the positive-going peak at higher wave number and the negative-going peak at lower wave number is observed. Further increased in the ORC treatment time to 50 min, a transformation from the bipolar band to a positive-going one, i.e., the anomalous IR absorption band, is witnessed. It is also noticed that along with the increase in the ORC treatment time, the intensity of CO_L band is enhanced significantly. These phenomena demonstrate that nanostructured Pt thin films exhibit anomalous IR properties.

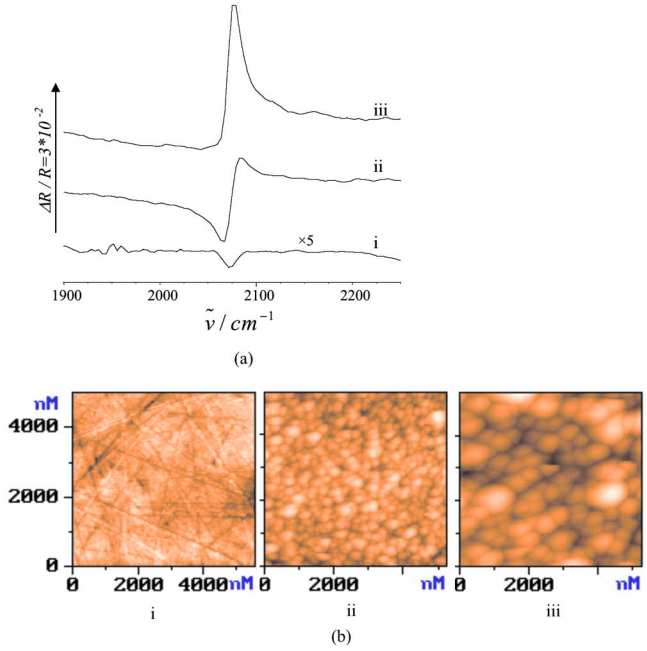

FIG. 3. (Color online) (a) *In situ* FTIR spectra of CO adsorbed on the nanostructured Pt thin films on Pt surface for different treatment time. (b) STM images of the corresponding thin films. The ORC treatment times are (i): 0 min, (ii) 20 min, and (iii) 50 min.

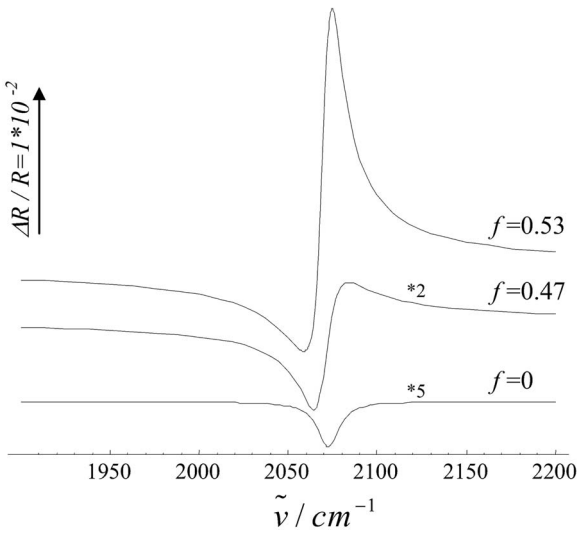

FIG. 4. Theoretical simulated spectra of CO adsorbed on the nanostructured Pt thin films on the Pt surface with variation in f using the Bruggeman EMT. The values of d_{eff} used in the simulation when f equals 0.47 and 0.53 are 36 and 142 nm, respectively.

In the IR experiment, there are also two instances to observe the special IR line shape. At low IR frequency region (250~400 cm^{-1}), the band of CO adsorbed on Cu(111) surface also exhibits an inverted band.[38,39] This phenomenon was named "antiabsorption" attributed to the frustrated (dipole-forbidden) rotational motion of chemisorbed CO. The other phenomenon concerning anomalous IR line shape is the "Christiansen effect," which was observed through the transmission IR experiments of organic molecules dispersed in KBr disks.[40,41] This effect can be explained by the difference between the refractive index of organic molecules and KBr. However, in our experiments, the reflection spectra were collected for CO molecules adsorbed on Pt nanomaterials and the anomalous IR band is located near 2070 cm^{-1}, which corresponds to the IR absorption of the stretching vibration mode of CO molecules. So the anomalous IR line shape observed in our experiment is different from the antiabsorption and from the Christiansen effect mentioned above. Therefore, in this paper, the term "anomalous IR features" observed on metal nanomaterials is used to distinguish from the term "normal IR features" observed on bulk metals.

Figure 3(b) illustrates the STM images of Pt thin films corresponding to the IR spectra in Fig. 3(a). Image (i) indicates that the untreated Pt surface is relatively smooth, except for some irregular scratches and defects caused by mechanical polishing. After 20 min of ORC treatment [image (ii)], island-shaped Pt nanoparticles appear on the Pt surface. The size of nanoislands is about tens of nanometers and some nanoparticles become aggregative. With further increased in the ORC treatment time, the nanoislands grow larger. After 50 min of ORC treatment [image (iii)], the size of nanoislands reaches 100~200 nm, but the aggregation degree of nanoparticles is analogical as that of image (ii). From Figs. 3(a) and 3(b), we can conclude that the features of IR spectra are transformed with the change in the Pt surface structure, demonstrating clearly correlations between the IR spectra and the structure of nanomaterials.

Figure 4 displays the theoretically simulated spectra of CO molecules adsorbed on the nanostructured Pt thin films with variation in f. In Eq. (3), as ε_m and ε_{mix} are the two parameters already known, ε_{eff} is only characterized by one single parameter f. The simulated spectra can be derived from ε_{eff}; hence, all the IR spectra are described by the parameter f. Such characteristic is convenient for us to compare the simulation results with the experimental data. In the simulation, as the intensity of CO band is directly proportional to the effective thickness of the second layer (d_{eff}),[37] we have to evaluate d_{eff} before simulation. Since the size of Pt nanoparticles is much larger than the length of CO molecules (0.175 nm), d_{eff} depends on the size of Pt hemisphere, which increases with the increase in the ORC treatment time (see the STM images). When the Pt surface is completely covered with a layer of Pt hemisphere, the roughness factor (R_r) of the Pt surface can be calculated as: $R_r = 2\pi r^2 / \pi r^2 = 2$, where r is the radius of Pt hemisphere. If the Pt nanoparticles are away from each other, the value of R_r will be smaller than 2, and if the Pt nanoparticles become aggregated, the value will exceed 2. This is confirmed by the cyclic voltammetry (CV) experiment that the largest roughness factor of the Pt surface only reaches 2.37. So d_{eff} can be evaluated approximately as: $d_{\text{eff}} = r \times R_r / 2$. Here R_r can be measured experimentally from CV curves according to the charge of hydrogen adsorption. The r can take the value of average size of Pt nanoparticles in nanostructured Pt films and can be measured from STM images (see supplementary material[42]).

It can be observed that when f equals 0, corresponding to mixed phase on bulk Pt surface, the IR spectrum of CO adsorbed is a normal IR absorption line, characterized by a negative-going band. With the increase in f, the IR spectra

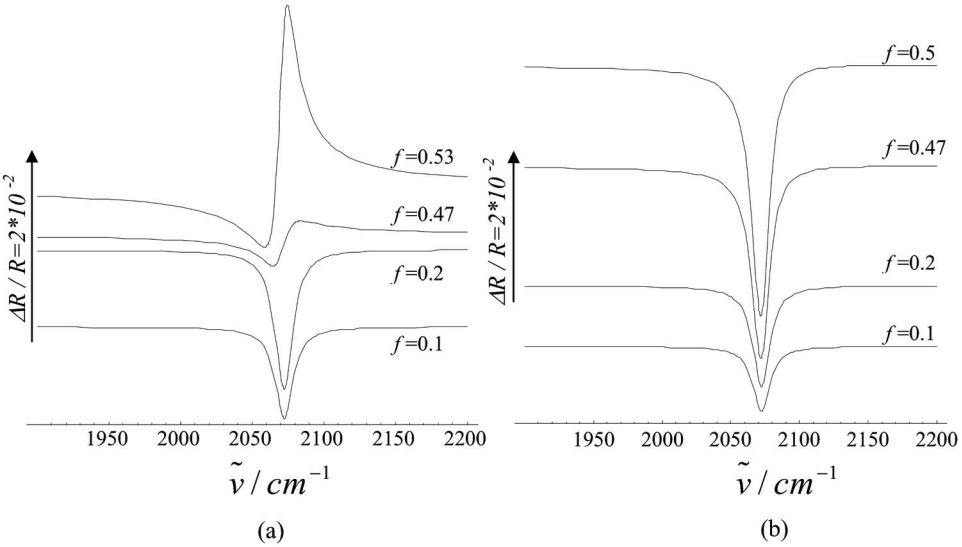

FIG. 5. Simulated IR spectra of CO adsorbed on the nanostructured Pt thin films using different models of EMT: (a) The Bruggeman model and (b) the MG model. d_{eff} used in the simulation are 10, 20, 36, and 142 nm, respectively, with the increase in f (the values are indicated in the figure).

change. When f equals 0.47, the CO band is transformed to a Fano-type bipolar band; when f increases further to 0.53, the direction of the CO band is inverted. d_{eff} is evaluated from the experimental data to be 36 and 142 nm, respectively, corresponding to the simulated IR spectra with f at 0.47 and 0.53. We have tested by simulation that if we fix the value of f and change d_{eff}, the shape of the simulated CO band remains unchanged, while the intensity of CO band augments with the increase in d_{eff}. On the same way, if we fix the value of d_{eff}, and make a small change in the value of f from 0.42 to 0.53, the shape of CO band changes from negative-going band to bipolar band and, finally, to positive-going band. This confirms clearly that f, the volume fraction of metal in the homogeneous medium, is a critical parameter. Furthermore, along with the variation of f, a fluctuation in the intensity of CO band could also be observed. However, this influence of f on the intensity of CO band is not significant in comparison with that of d_{eff} variation. In the experiment, with the increase in the ORC treatment time, although the size of Pt nanoislands becomes larger, the increase in aggregation degree of nanoparticles is not significant. Accordingly, in the simulation, d_{eff} increases significantly, while the value of f has only a minor increase. So we can conclude that the shape of IR band is dependent on the value of f, which may be related directly to the aggregation degree of nanoparticles; while the intensity of IR band is directly proportional to d_{eff}, which depends on the size of nanoislands. By comparing the experimental data with the simulation results, it can be demonstrated that with the increase in the ORC treatment time, the values of d_{eff} and f increase, so the IR spectra are transformed accordingly from normal IR absorption to Fano-type bipolar band and finally to anomalous IR absorption.

It is worthwhile to note that in our simulation, we have used different optical constants of metal as the substrate layer, but the simulation results are similar; and we have also tested that the features of the CO band have not been affected by using either air (refractive index: 1) or water (refractive index: $1.316-0.016\times i$) as the top layer.

It is interesting to note that different models of EMT sometimes may lead to different results.[43] Figures 5(a) and 5(b) illustrate the simulated IR spectra of CO adsorbed on the nanostructured Pt thin films using the Bruggeman (Br) model and the MG model of EMT, respectively. It should be noticed nevertheless that the MG model is unsuitable when f is bigger than 0.5,[29] so that the simulation of MG model only reaches f value of 0.5. It can be found that, in the Br model, with the increase in f, the CO band is transferred from normal IR absorption to Fano-type bipolar band and, finally, to anomalous IR absorption band, in accordance with the experimental data. However, as shown in Fig. 5(b), the CO band obtained using the MG model is always normal with different values of f. Granqvist and Hunderi[28] and Osawa *et al.*[20] explained that the MG model only included Lorentz field, but the Br model, as a mean-field theory, had taken into account the particle interactions as a constant far field. By comparing the simulation results of two models, we can conclude that the interactions between Pt and Pt islands as well as those between Pt and CO molecules are responsible for the specific IR line shape.[17,20] Such interactions are nevertheless neglected in the MG model.

In this paper, the three peculiar IR line shapes observed experimentally on nanomaterials can be explained by the same model by changing the value of f, which implies that the SEIRA, the Fano-type, and the AIREs could belong to the same origin. From the simulation, it is observed that the features of IR spectra vary drastically with the increase in f. As a further study, the investigation of calculating the value of f for different nanostructures is in progress.

IV. CONCLUSION

In the current paper, a simple EMT is introduced into a three-layer model in simulating the anomalous IR spectra of CO adsorbed on the nanostructured Pt films. The results demonstrate that the CO band is transformed from normal IR absorption to Fano-type bipolar band and, finally, to the enhanced anomalous IR absorption band with the increase in f (the volume fraction of metal in the composite system) and d_{eff} (the effective thickness of the composite system). The simulation results have well interpreted the experimental

data. The differences in simulation using the Bruggeman model of EMT and the MG model of EMT revealed that the interactions between Pt and Pt nanoparticles as well as between Pt and CO molecules are the possible origin of anomalous IR properties. From the STM and simulation results, we have concluded that the spectral line shape of IR absorption is strongly dependent on f, which is related directly to the aggregation degree of nanoparticles; while the intensity of IR band is directly proportional to d_{eff}, which depends on the size of nanoislands. Although experimental data evidenced three distinct IR features, i.e., the SEIRA, the Fano-type, and the AIREs observed for the anomalous IR properties of nanomaterials, the present paper demonstrates that they can be explained through the same model just by changing the value of f, and reveals that they may belong to the same origin.

ACKNOWLEDGMENTS

This work was supported by grants from the National Natural Science foundation of China (20673091) and Ministry of Science and Technology (2002CB211804 and 2007DFA40890).

[1] C. Burda, X. B. Chen, R. Narayanan, and M. A. El-Sayed, Chem. Rev. (Washington, D.C.) **105**, 1025 (2005).
[2] M. C. Daniel and D. Astruc, Chem. Rev. (Washington, D.C.) **104**, 293 (2004).
[3] N. Tian, Z.-Y. Zhou, S.-G. Sun, Y. Ding, and Z.-L. Wang, Science **316**, 732 (2007).
[4] A. Hartstein, J. R. Kirtley, and J. C. Tsang, Phys. Rev. Lett. **45**, 201 (1980).
[5] Z.-Q. Tian, B. Ren, and D.-Y. Wu, J. Phys. Chem. B **106**, 9463 (2002).
[6] G.-Q. Lu, S.-G. Sun, L.-R. Cai, S.-P. Chen, Z.-W. Tian, and K.-K. Shiu, Langmuir **16**, 778 (2000).
[7] S.-G. Sun, in *Catalysis and Electrocatalysis at Nanoparticle Surfaces*, edited by A. Wieckowski, E. Savinova, and C. G. Vayenas (Dekker, New York, 2003), Chap. 21, pp. 785–826.
[8] A. E. Bjerke, P. R. Griffiths, and W. Theiss, Anal. Chem. **71**, 1967 (1999).
[9] M.-S. Zheng and S.-G. Sun, J. Electroanal. Chem. **500**, 223 (2001).
[10] W.-G. Lin, S.-G. Sun, Z.-Y. Zhou, S.-P. Chen, and H.-C. Wang, J. Phys. Chem. B **106**, 11778 (2002).
[11] H. Gong, S.-G. Sun, J.-T. Li, Y.-J. Chen, and S.-P. Chen, Electrochim. Acta **48**, 2933 (2003).
[12] H.-C. Wang, S.-G. Sun, J.-W. Yan, H.-Z. Yang, and Z.-Y. Zhou, J. Phys. Chem. B **109**, 4309 (2005).
[13] Q.-S. Chen, S.-G. Sun, J.-W. Yan, J.-T. Li, and Z.-Y. Zhou, Langmuir **22**, 10575 (2006).
[14] G. Orozco and C. Gutierrez, J. Electroanal. Chem. **484**, 64 (2000).
[15] R. Ortiz, A. Cuesta, O. P. Marquez, J. Marquez, J. A. Mendez, and C. Gutierrez, J. Electroanal. Chem. **465**, 234 (1999).
[16] U. Fano, Phys. Rev. **124**, 1866 (1961).
[17] A. Priebe, M. Sinther, G. Fahsold, and A. Pucci, J. Chem. Phys. **119**, 4887 (2003).
[18] Y. Zhu, H. Uchida, and M. Watanabe, Langmuir **15**, 8757 (1999).
[19] D. A. Heaps and P. R. Griffiths, Vib. Spectrosc. **42**, 45 (2006).
[20] M. Osawa, K. Ataka, K. Yoshii, and Y. Nishikawa, Appl. Spectrosc. **47**, 1497 (1993).
[21] M. Osawa, Bull. Chem. Soc. Jpn. **70**, 2861 (1997).
[22] H. Gong, S.-G. Sun, Y.-J. Chen, and S.-P. Chen, J. Phys. Chem. B **108**, 11575 (2004).
[23] Y.-J. Chen, S.-G. Sun, S.-P. Chen, J.-T. Li, and H. Gong, Langmuir **20**, 9920 (2004).
[24] J. C. Maxwell-Garnett, Philos. Trans. R. Soc. London **203**, 385 (1904).
[25] A. G. Bruggeman, Ann. Phys. (Leipzig) **24**, 636 (1935).
[26] H. Starke, C. Johnston, S. Hill, P. Dobson, and P. S. Grant, J. Phys. D **39**, 1305 (2006).
[27] R. Chang, H.-P. Chiang, P. T. Leung, D. P. Tsai, and W. S. Tse, Solid State Commun. **133**, 315 (2005).
[28] G. Granqvist and O. Hunderi, Phys. Rev. B **18**, 2897 (1978).
[29] W. Cohen, G. D. Cody, M. D. Coutts, and B. Abeles, Phys. Rev. B **8**, 3689 (1973).
[30] S. Toyama, O. Takei, M. Tsuge, and R. Usami, Electrochem. Commun. **4**, 540 (2002).
[31] E. Johnson and R. Aroca, J. Phys. Chem. **99**, 9325 (1995).
[32] C. Pecharroman, A. Cuesta, and C. Gutierrez, J. Electroanal. Chem. **563**, 91 (2004).
[33] C.-X. Wu, H. Lin, Y.-J. Chen, W.-X. Li, and S.-G. Sun, J. Chem. Phys. **121**, 1553 (2004).
[34] J. E. Bertie, M. K. Ahmed, and H. H. Eysel, J. Phys. Chem. **93**, 2210 (1989).
[35] D. W. Lynch and W. R. Hunter, in *Handbook of Optical Constants of Solids*, edited by E. D. Palik (Academic, Orlando, 1985), pp. 333–342.
[36] X. Zhang and D. Stroud, Phys. Rev. B **52**, 2131 (1995).
[37] J. D. E. McIntyre, in *Advances in Electrochemistry and Electrochemical Engineering*, edited by R. H. Muller (Wiley, New York, 1973), Vol. 9, pp. 61–166.
[38] P. Dumas, M. Hein, A. Otto, B. N. J. Persson, P. Rudolf, R. Rava, and G. P. Williams, Surf. Sci. **433–435**, 797 (1999).
[39] C. J. Hirschmugl and G. P. Williams, Phys. Rev. B **52**, 14177 (1995).
[40] H. J. Hoffmann, Appl. Phys. B: Lasers Opt. **70**, 853 (2000).
[41] X.-D. Liu, L.-T. Hou, and H.-T. Wang, Infrared Phys. Technol. **43**, 401 (2002).
[42] See EPAPS Document No. E-JCPSA6-129-805828 for the estimation of the effective thickness of the second layer. For more information on EPAPS, see http://www.aip.org/pubservs/epaps/html.
[43] J. I. Gittleman and B. Abeles, Phys. Rev. B **15**, 3273 (1977).